Geol. Mag. **139** (5), *2002, pp. 525–539. © 2002 Cambridge University Press*
DOI: 10.1017/S001675680200674X *Printed in the United Kingdom*

159 Ma Kjakebeinet lamproites (Dronning Maud Land, Antarctica) and their implications for Gondwana breakup processes

A. V. LUTTINEN*, X. ZHANG† & K. A. FOLAND†

*British Antarctic Survey, High Cross, Madingley Road, Cambridge CB3 0ET, UK
†Department of Geological Sciences, Ohio State University, Columbus, OH 43210, USA

(*Received* 25 July 2001; *accepted* 10 May 2002)

Abstract – Lamproite dykes that cross-cut Middle Jurassic Karoo-related flood basalts in Vestfjella, Dronning Maud Land, Antarctica, have been dated at 158.7 ± 1.6 Ma by $^{40}Ar/^{39}Ar$ incremental heating of phlogopite. Compared to most lamproites, these dykes are unusually low in SiO_2 (40.09–40.18 wt %) and high in CaO (12.35–16.24 wt %) and P_2O_5 (3.03–3.81 wt %). They have broad affinities to spatially and temporally related group II kimberlites of southern Africa, but the geochemically closest correlatives are CaO- and P_2O_5-rich diopside madupitic lamproites from Leucite Hills, USA. The Kjakebeinet lamproites are notably high in incompatible elements, show negative initial ε_{Nd} values (–6.0, –6.7) and positive initial ε_{Sr} values (+14, +17) with T_{DM} model ages of *c.* 1.1 Ga, and probably record melting of metasomatized subcontinental lithospheric mantle beneath western Dronning Maud Land. Their emplacement records the youngest recognized magmatic event in the region, coincides with the proposed second and final stage of Gondwana breakup between Africa and Antarctica, and may be associated with deep-seated coast-parallel strike-slip faulting in Dronning Maud Land. Survival of old, easily fusible lithospheric mantle material 20 Ma after the eruption of voluminous flood basalt magmas suggests that the latter were emplaced within narrow zones of lithospheric thinning and that the source of lamproites remained largely intact between these zones.

Key words: lamproite, Gondwana, Ar/Ar, geochronology, isotopes, Antarctica.

1. Introduction

The Jurassic breakup of Gondwana was associated in western Dronning Maud Land, Antarctica, with eruptions of voluminous continental flood basalt lavas. Recent dating by $^{40}Ar/^{39}Ar$ methods suggests their emplacement was synchronous, or nearly so, with basaltic magmatism in southeastern Africa (the Karoo province) and along the Transantarctic Mountains (the Ferrar province) and occurred during a short period at *c.* 177–184 Ma (Heimann *et al.* 1994; Fleming *et al.* 1997; Duncan *et al.* 1997; X. Zhang, pers. comm., 2002). Eruption of the basalts and intrusion of widespread coast-parallel dolerites in western Dronning Maud Land and southeastern Africa have been associated with lithospheric extension during the initial stage of Gondwana breakup (Cox, 1992; Grantham, 1996). The peak of tholeiitic magmatism significantly preceded the final breakup, as the oldest identified seafloor anomaly between East and West Gondwana (M25 in the Somali Basin: Rabinowitz, Coffin & Falvey, 1983) has been dated at 156–157 Ma (Gradstein *et al.* 1995). However, it has been suggested that the seafloor spreading began before 160 Ma (Lavwer, Gahagan & Coffin, 1992; Livermore & Hunter, 1996; Roeser, Fritsch & Hinz, 1996). In southeastern Africa and western Dronning Maud Land, the beginning of seafloor spreading in the Somali Basin marks a change from E–W stretching to coast-parallel displacements generated by transform faulting (Cox, 1992). Geological evidence of this stage has been lacking in Dronning Maud Land and little is known about the events that finally led to development of a mid-ocean ridge system between Africa and Antarctica.

During the Finnarp (Finnish Antarctic Research Program) 1997 expedition, a minor suite of lamproite dykes was discovered. The dykes cross-cut the flood basalt lavas and associated tholeiitic intrusive rocks of southern Vestfjella, Dronning Maud Land. Here, in this first report of lamproites in Dronning Maud Land, the results of $^{40}Ar/^{39}Ar$ dating, Nd and Sr isotopic and chemical analyses are presented. The isotopic and chemical data for the lamproites constrain the age and composition of the upper mantle of Dronning Maud Land and provide new insights to the regional breakup processes.

2. Geological background

The geological record of western Dronning Maud

* Author for correspondence: arto.luttinen@helsinki.fi; present address: Department of Geology, P.O. Box 64, 00014-University of Helsinki, Finland

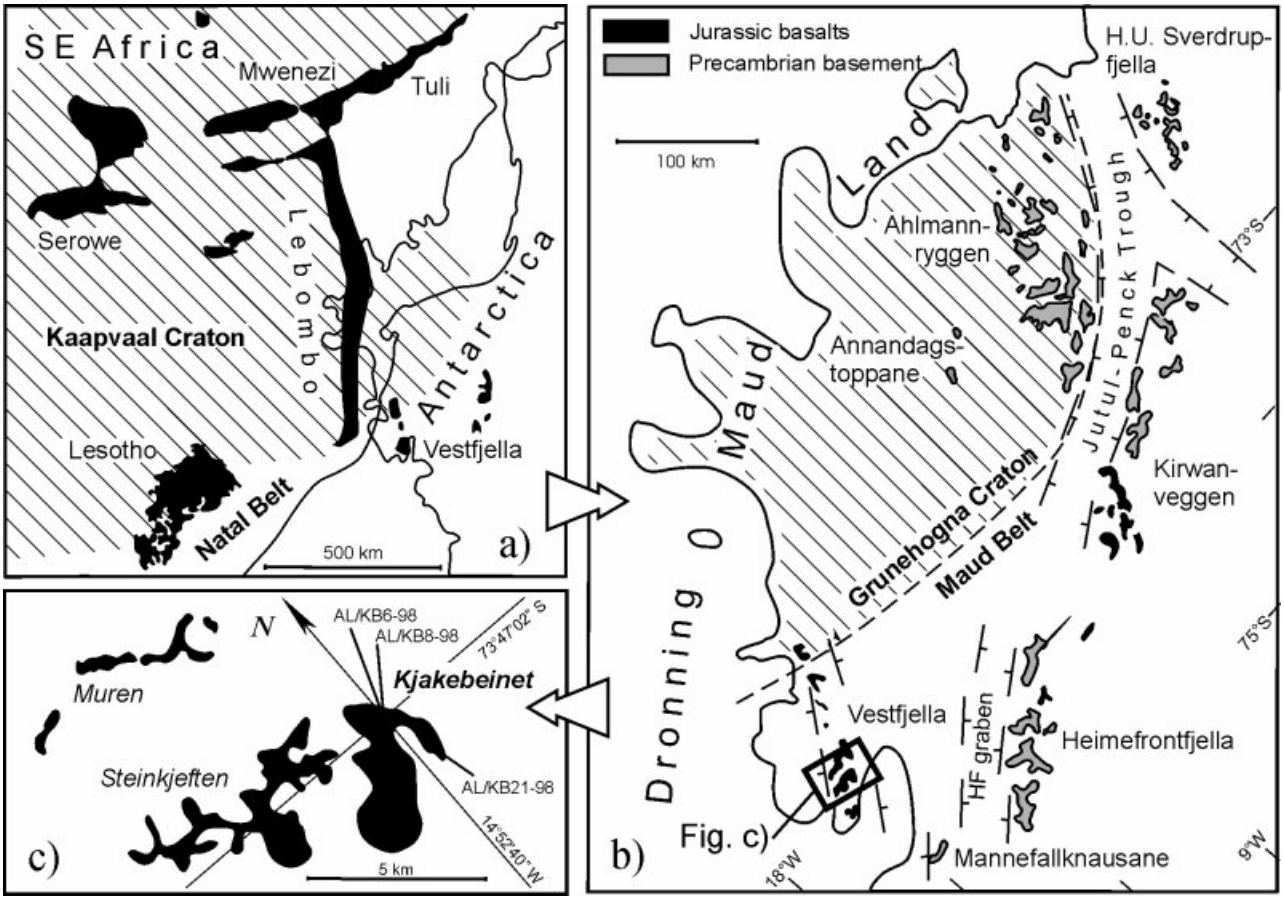

Figure 1. Distribution of Jurassic Karoo-related flood basalts, Archaean cratons (hatching), and Proterozoic basement in (a) southeastern Africa and (b) western Dronning Maud Land. Lamproite sample localities are depicted in (c). Reconstruction of Gondwana is after Lawver, Gahagan & Coffin (1992).

Land demonstrates a long common history with southeastern Africa. The basement rocks of the Archaean Grunehogna Craton and the Mesoproterozoic Maud Belt of Dronning Maud Land have equivalents in the Kaapvaal Craton and the Natal Belt, respectively (Fig. 1) (e.g. Wolmarans & Kent, 1982; Jacobs, Thomas & Weber, 1993). In both areas, Palaeozoic sedimentary rocks overlie the basement and Mesozoic flood basalts cap the Gondwanan stratigraphy. Geochemical similarities have confirmed that the *c.* 180 Ma flood basalts of Dronning Maud Land represent an Antarctic extension of the Karoo large igneous province (Harris *et al.* 1990; Luttinen & Furnes, 2000).

Remains of the Jurassic basaltic succession occur along the East Antarctic plateau escarpment (Kirwanveggen and Heimefrontfjella) and comprise the bedrock of Vestfjella near the continental margin (Fig. 1b). Luttinen & Furnes (2000) linked generation of the various tholeiitic magma types of Vestfjella (Luttinen & Siivola, 1997; Luttinen, Rämö & Huhma, 1998) to regions of lithospheric thinning and proposed that the eruptions were focused on two zones. One of these is represented by the Jutul-Penck and Heimefrontfjella grabens (Fig. 1b) and the other was located where the present continental margin marks the site of Jurassic lithospheric splitting. Several volumetrically minor alkaline plutons crop out in the vicinity of the Jutul-Penck zone and have been associated with its development at about 170–180 Ma (Harris & Grantham, 1993; Grantham, 1996). Some of them are cross-cut by various silica over- and undersaturated dyke rocks including microgranites, nephelinites, and 'lamprophyric' types (Harris & Grantham, 1993).

Intrusive equivalents of flood basalts are mainly dolerite dykes, which are widespread in western Dronning Maud Land (Juckes, 1972; Spaeth & Schüll, 1987; Peters, 1989; Harris, Watters & Groenewald, 1991). They are quite rare in Kirwanveggen and Heimefrontfjella, but fairly abundant in Ahlmannryggen and their abundance appears to increase toward Vestfjella (Spaeth & Schüll, 1987), where recent mapping of NE-trending dykes at Muren (Fig. 1c) indicates up to 14% upper crustal extension (S. Vuori, pers. comm., 2001). Other, subordinate regional dyke orientations are NW–SE and E–W (Spaeth & Schüll, 1987; Grind, Luttinen & Siivola, 1991). Two Jurassic gabbroic plutons associate with the zone of high dyke frequency in southern Vestfjella (S. Vuori, pers. comm., 2001).

https://doi.org/10.1017/S001675680200674X Published online by Cambridge University Press

Three macroscopically distinctive mica-rich mafic dykes with a 'lamprophyric' field-appearance cross-cut basalts and dolerites at Kjakebeinet, an isolated nunatak toward the southern end of Vestfjella (Fig. 1c). These dykes record a previously unreported rock type in Vestfjella and their occurrence seems to be confined to this locality. The dykes are *c.* 1 m wide, subvertical and exhibit a general N–S strike but in places, for short distances, follow the NE- and NW-trending dolerites. The mica-rich dykes contain scattered, small leucocratic clots and felsic xenoliths. Boulders of the 'lamprophyric' rock type occur on scree below the summit. These contain abundant and well-rounded xenoliths of various crustal rock types.

3. Samples and methods

Analysed samples AL/KB6-98, AL/KB8-98 and AL/KB21-98 are from the cores of three mica-rich dykes. The former two have been collected from the summit of Kjakebeinet (73°47'02"N, 14°52'40"W), whereas the third sample is from a dyke that is located about 2 km south of the summit (Fig. 1c). It is currently unclear whether the latter represents an extension of one of the dykes at the summit or not.

3.a. Mineralogy and classification

The fine-grained mica-rich mafic dykes of Kjakebeinet have an aphyric field-appearance, but contain sparse clinopyroxene phenocrysts (< 2.5 mm) and talc pseudomorphs after olivine (< 2.0 mm).

Talc replacement of olivine (1–5 vol. %) is universal. Judging from their shape, some of the pseudomorphs represent altered euhedral olivine phenocrysts, whereas the others may replace rounded and anhedral olivine macrocrysts. Clinopyroxene phenocrysts (*c.* 1 vol. %) are euhedral, nearly colourless and have diopsidic compositions from the core to the rim. Seriate, pale yellow-brown to red-brown pleochroic, euhedral, and TiO_2-rich (3.32–6.64 wt %) phlogopite is the predominant mineral (*c.* 30–40 vol. %). Electron microprobe analyses show wide compositional ranges from phlogopitic cores to rims approaching Ti-rich tetraferriphlogopite. Nearly Na-free potassium feldspar (sanidine?) (*c.* 10–15 vol. %), Na- and Al-poor diopside (*c.* 10–15 vol. %), dolomitic carbonate (*c.* 10–15 vol. %), and apatite (*c.* 5 %) comprise the groundmass together with minor aegirine–augite and accessory Fe–Ti oxide, Cr-spinel, pyrite, barite, quartz, rutile, Th-REE-phosphate (monazite), and zircon. Carbonate and sanidine occur interstitially, but typically are concentrated in leucocratic globular aggregates, which grade from sharply defined subspherical ocelli to vague patches, barely differentiated from their host. On the basis of their modal and mineralogical compositions and the mode of occurrence, the Kjakebeinet dykes can be classified as lamproite (Woolley *et al.* 1996). The presence of monazite and abundant carbonate are atypical of lamproites, however (Mitchell & Bergman, 1991).

3.b. $^{40}Ar/^{39}Ar$ measurements

Phlogopite grains were separated using a magnetic separator and careful paper-shaking from the 0.125 mm to 0.25 mm sieve fraction. The separates were washed in an ultrasonic water bath after which they looked pure, clean and moderately fresh.

The $^{40}Ar/^{39}Ar$ measurements were performed at the Ohio State University, using general laboratory procedures that have been described previously (Foland *et al.* 1993), except for the use of a new noble-gas mass analysis system. Aliquots of 2 to 4 mg of phlogopite were irradiated in the L-67 position of Ford Nuclear Reactor, Phoenix Memorial Laboratory, at the University of Michigan, for 36 hours. They were subsequently analysed incrementally by heating to successively higher temperatures using a custom-built resistance-heating, low-blank furnace. The step heating was continuous with ramp times from one temperature to another of about a minute and with dwell times of about 30 minutes at each temperature. These incremental-heating fractions were analysed by static gas mass analysis with a MAP 215-50 mass spectrometer, in about 30 steps. The monitor used was an intralaboratory muscovite standard ('PM-1') with a $^{40}Ar/^{39}Ar$ age of 165.3 Ma; an uncertainty of ± 1 % is assigned to this age in order to allow for uncertainties in the standards against which PM-1 was calibrated. The age for this monitor was determined by simultaneous cross-calibration with several monitors including the Fish Canyon Tuff biotite standard (FCT-3) with an age of 27.84 (± 0.08) Ma. The uncertainties quoted for plateau ages do not include provision for the systematic uncertainty in the monitor age. Corrections for interfering reactions producing Ar from K, Ca and Cl were made by factors determined using K_2SO_4 and CaF_2 salts, and wollastonite ($CaSiO_3$) irradiated at the same time.

3.c. Geochemical and Nd and Sr isotopic analyses

The dykes were analysed for major, minor and trace elements using X-ray fluorescence (XRF) and an inductively coupled plasma source mass spectrometer (ICP-MS) at the Geoanalytical Laboratory, Washington State University. Detailed descriptions of the analytical procedure, precision and accuracy of the XRF and ICP-MS analyses have been given by Johnson, Hooper & Conrey (1999) and Knaack, Cornelius & Hooper (1994), respectively. XRF measurements were performed on ignited (1000 °C) powders. Loss on ignition (LOI) was also determined using a temperature of 1200 °C at the Geochemical Laboratory, Department of Geology, University of Helsinki. Overall, the data for international rock

https://doi.org/10.1017/S001675680200674X Published online by Cambridge University Press

Table 1. $^{40}Ar/^{39}Ar$ analytical results for phlogopite separates from Kjakebeinet lamproites

T [a]	^{40}Ar [b] / ^{39}Ar	^{38}Ar [b] / ^{39}Ar	^{37}Ar [b] / ^{39}Ar	^{36}Ar [b] / ^{39}Ar	F [c] (%)	^{39}Ar [d] (%)	$^{40}Ar^*$ [e]	K/Ca [f]	K/Cl [g]	Apparent Age (Ma) [h]
AL/KB8-98 phlogopite, no. 64K20 (J = 0.05595, wt = 3.48 mg, %K = 7.55)										
600	16.94	0.0399	1.488	1.756	11.86	1.06	70.0	0.351	210	115.9 ± 0.7
651	20.31	0.0296	3.913	1.555	16.05	0.88	78.9	0.133	348	155.1 ± 0.7
680	18.20	0.0216	1.044	0.6325	16.40	0.97	90.2	0.500	604	158.4 ± 0.6
701	47.78	0.0375	0.2034	10.46	16.88	0.99	35.3	2.57	857	162.8 ± 2.0
721	24.00	0.0193	0.0684	2.391	16.92	1.39	70.6	7.64	1720	163.2 ± 0.7
741	20.03	0.0161	0.0407	1.064	16.87	2.05	84.3	12.8	2240	162.7 ± 0.5
760	17.11	0.0137	0.0315	0.1592	16.62	3.13	97.3	16.6	3150	160.4 ± 0.3
781	16.85	0.0139	0.0261	0.1045	16.52	4.25	98.2	20.1	2610	159.5 ± 0.3
800	16.82	0.0138	0.0204	0.0946	16.53	4.92	98.3	25.6	2840	159.5 ± 0.3
821	16.73	0.0137	0.0171	0.0739	16.49	5.57	98.7	30.5	2910	159.2 ± 0.3
840	16.64	0.0134	0.0155	0.0578	16.45	6.82	99.0	33.7	3340	158.9 ± 0.3
861	16.66	0.0135	0.0156	0.0640	16.45	7.41	98.9	33.6	3200	158.9 ± 0.3
881	16.72	0.0142	0.0229	0.1096	16.38	7.42	98.1	22.8	2360	158.2 ± 0.4
901	16.76	0.0144	0.0264	0.1177	16.40	7.65	97.9	19.8	2160	158.4 ± 0.4
921	16.82	0.0137	0.0291	0.1143	16.47	7.21	98.0	18.0	2960	159.0 ± 0.3
941	16.92	0.0135	0.0385	0.1431	16.48	5.63	97.5	13.6	3540	159.1 ± 0.3
956	16.94	0.0139	0.0412	0.1644	16.44	4.51	97.1	12.7	2890	158.8 ± 0.3
970	16.82	0.0136	0.0424	0.1325	16.41	3.51	97.7	12.3	3170	158.5 ± 0.3
980	16.87	0.0137	0.0463	0.1244	16.48	2.81	97.8	11.3	2970	159.2 ± 0.4
991	16.85	0.0139	0.0570	0.1202	16.48	2.48	97.9	9.17	2660	159.1 ± 0.4
1000	16.75	0.0141	0.0680	0.1230	16.38	2.11	97.9	7.69	2420	158.2 ± 0.4
1021	16.83	0.0139	0.0819	0.1150	16.48	3.00	98.0	6.39	2690	159.1 ± 0.3
1040	16.83	0.0143	0.1015	0.1373	16.41	3.43	97.6	5.15	2270	158.5 ± 0.3
1073	16.95	0.0149	0.1541	0.1847	16.39	4.29	96.8	3.39	1890	158.3 ± 0.3
1102	17.21	0.0169	0.3569	0.2811	16.40	3.09	95.3	1.47	1130	158.3 ± 0.4
1152	17.37	0.0234	0.9128	0.3631	16.36	2.05	94.2	0.573	474	158.0 ± 0.4
1202	17.49	0.0275	1.829	0.3827	16.50	1.02	94.4	0.286	347	159.3 ± 0.6
1351	19.51	0.0510	5.590	1.211	16.42	0.31	83.9	0.093	140	158.6 ± 1.5
1501	32.00	0.0409	2.227	5.367	16.33	0.05	51.0	0.234	272	157.7 ± 8.2
Integrated	17.37	0.0153	0.1650	0.3206	16.42	100	94.6	3.17	1780	158.5
781–1102°C		(86% of ^{39}Ar)							158.8 ± 0.4	
AL/KB21-98, no. 64K23 (J = 0.05604, wt = 1.81 mg, %K = 8.77)										
600	17.45	0.0390	1.027	1.564	12.90	0.62	74.0	0.509	214	125.9 ± 1.4
666	20.82	0.0243	2.791	1.508	16.59	0.78	79.6	0.187	535	160.4 ± 1.2
691	18.04	0.0193	0.8088	0.6292	16.24	0.89	90.0	0.646	824	157.1 ± 0.9
700	17.56	0.0179	0.1330	0.4135	16.33	0.88	93.1	3.93	973	158.0 ± 0.8
721	45.91	0.0334	0.0442	9.810	16.90	1.50	36.8	11.8	1650	163.3 ± 2.1
741	18.65	0.0152	0.0228	0.7052	16.55	2.67	88.8	22.9	2420	160.0 ± 0.5
760	16.77	0.0134	0.0151	0.1078	16.44	4.88	98.1	34.7	3500	159.0 ± 0.3
781	16.62	0.0137	0.0103	0.0568	16.43	8.14	99.0	50.5	2830	158.9 ± 0.3
801	16.49	0.0135	0.0079	0.0313	16.38	8.67	99.4	66.6	3090	158.4 ± 0.3

820	16.52	0.0136	0.0079	0.0464	16.36	7.72	99.2	66.1	2920	158.3 ± 0.3
840	16.57	0.0138	0.0094	0.0553	16.39	6.71	99.0	55.7	2620	158.5 ± 0.3
860	16.73	0.0140	0.0130	0.1012	16.41	5.86	98.2	40.2	2480	158.7 ± 0.3
880	17.81	0.0148	0.0208	0.4573	16.44	8.58	92.4	25.1	2410	159.0 ± 0.3
890	17.62	0.0145	0.0252	0.4143	16.38	4.99	93.1	20.7	2600	158.5 ± 0.4
900	17.13	0.0141	0.0277	0.2239	16.46	2.58	96.1	18.9	2650	159.1 ± 0.4
910	16.90	0.0138	0.0297	0.1547	16.43	1.83	97.3	17.6	3010	158.9 ± 0.5
920	16.77	0.0134	0.0331	0.1352	16.36	1.53	97.6	15.8	3650	158.2 ± 0.5
930	16.71	0.0144	0.0377	0.1014	16.39	1.34	98.2	13.9	2120	158.5 ± 0.6
940	16.71	0.0140	0.0386	0.1273	16.31	1.28	97.8	13.6	2560	157.8 ± 0.6
951	16.74	0.0142	0.0425	0.0989	16.44	1.34	98.3	12.3	2340	159.0 ± 0.6
966	16.71	0.0143	0.0468	0.0955	16.42	1.61	98.3	11.2	2240	158.8 ± 0.5
981	16.77	0.0141	0.0521	0.1113	16.43	1.51	98.1	10.0	2480	158.9 ± 0.5
1001	16.72	0.0147	0.0605	0.0981	16.42	1.87	98.3	8.64	1870	158.8 ± 0.4
1022	16.64	0.0143	0.0713	0.0864	16.37	2.99	98.5	7.34	2180	158.3 ± 0.4
1041	16.69	0.0144	0.0880	0.0887	16.42	2.94	98.5	5.95	2080	158.8 ± 0.4
1061	16.75	0.0149	0.1150	0.1300	16.36	2.85	97.8	4.55	1820	158.2 ± 0.4
1101	16.93	0.0157	0.1881	0.1652	16.44	4.96	97.2	2.78	1420	159.0 ± 0.4
1154	16.92	0.0185	0.4427	0.1806	16.41	4.62	97.1	1.18	819	158.7 ± 0.3
1202	16.82	0.0190	0.5342	0.1982	16.27	2.44	96.8	0.979	758	157.4 ± 0.4
1351	17.16	0.0236	0.9459	0.3206	16.27	1.29	94.9	0.553	461	157.5 ± 0.6
1504	24.65	0.0248	0.7187	2.775	16.49	0.13	66.9	0.727	666	159.5 ± 4.8
Integrated	17.41	0.0152	0.1151	0.3409	16.39	100	94.3	4.54	1850	158.5
Plateau: 781–1154°C		(89% of ^{39}Ar)								158.6 ± 0.4

[a] Temperature in °C measured with a thermocouple on the outside of the Ta furnace crucible.
[b] The isotope ratios given are not corrected for Ca, K and Cl derived Ar isotopic interference but, ^{37}Ar is corrected for decay using a half-life of 35.1 days. The ratios are corrected for line blanks and mass discrimination.
[c] F is the ratio of radiogenic ^{40}Ar to K-derived ^{39}Ar. It is corrected for atmospheric argon and other nuclear reactions using the following factors:
$^{40}Ar/^{36}Ar)_{air} = 295.5$
$^{38}Ar/^{39}Ar)_K = 0.01175$
$^{38}Ar/^{37}Ar)_{Ca} = 3.500 \times 10^{-5}$
$^{36}Ar/^{38}Ar)_{Cl} = 2.018 \times 10^{-6}$ per day after irradiation.
$^{39}Ar/^{37}Ar)_{Ca} = 6.765 \times 10^{-4}$
$^{36}Ar/^{37}Ar)_{Ca} = 2.683 \times 10^{-4}$
$^{40}Ar/^{39}Ar)_K = 0.02050$
[d] Relative percent of the total ^{39}Ar released in the fraction. The K concentration given for each sample is the wt% of potassium in the bulk separate, determined by the the total quantity of ^{39}Ar produced during neutron irradiation and released during incremental-heating analysis.
[e] Percent of the total ^{40}Ar in the fraction that is radiogenic.
[f] Weight ratio calculated using the relationship: $K/Ca = 0.523 \times {}^{39}ArK/{}^{37}ArCa)$.
[g] Weight ratio calculated using the relationship: $K/Cl = 5.220 \times {}^{39}ArK/{}^{38}ArCl)$.
[h] Ages calculated with a total decay constant of 5.543×10^{-10} y^{-1}. 'Integrated' indicates the calculated summation for all fractions combined. 'Plateau' gives the values calculated for the age plateau fractions, where "% ^{39}Ar" is the percentage of total ^{39}Ar in the plateau fractions. All uncertainties are given at the one-sigma level. For increments of a step-heating analysis, the uncertainties do not include any J value uncertainty. For plateau ages, uncertainties reflect a relative uncertainty of ± 0.25% in J value. An overall systematic uncertainty of ±1% is assigned to all ages to allow for uncertainty in the monitor age. The monitor used was a intralaboratory muscovite standard ("PM-1") that has a ^{40}Ar/^{39}Ar age of 165.3 Ma; an uncertainty of ± 1% is assigned to this age in order to allow for uncertainties in the standards against which PM-1 was calibrated. The age for this monitor was determined by simultaneous cross calibration with several monitors including the Fish Canyon Tuff biotite standard (FCT-3) with an age of 27.84 Ma.

standards analysed at the Geoanalytical Laboratory conform quite well to values obtained using various methods in other laboratories (Johnson, Hooper & Conrey, 1999; Knaack, Cornelius & Hooper, 1994).

The isotopic analyses were performed at the Unit for Isotope Geology, Geological Survey of Finland. The rock powders (170–200 mg for Nd and Sr) were spiked with ^{149}Sm–^{150}Nd and ^{87}Rb–^{84}Sr tracers and dissolved in molded Teflon vials in a 1 : 4 mixture of HNO_3 and HF. After evaporation the samples were dissolved in HCl. Rubidium, strontium and light rare earth elements (LREE) were separated using standard cation exchange chromatography. Samarium and neodymium were purified on quartz columns following the method of Richard, Shimizu & Allègre (1976). The total procedural blanks were < 250 pg for both Nd and Sr. Isotope ratios of Sm, Nd and Sr were measured on a VG Sector 54 mass spectrometer (those of Nd and Sr in dynamic mode). Isotopic measurements on Rb were performed using a non-commercial Nier-type mass spectrometer built at the Geological Survey of Finland. Repeated analyses of La Jolla Nd standard gave $^{143}Nd/^{144}Nd$ of 0.511849 ± 0.000011 (mean and external 2σ error of eleven measurements); external error in the reported ^{143}Nd–^{144}Nd ratios is estimated to be better than 0.0025%. Repeated analyses of NBS987 Sr standard gave $^{87}Sr/^{86}Sr$ of 0.710258 ± 0.000026 (mean and external 2σ error of twelve measurements). The external error in the reported ^{87}Sr–^{86}Sr ratios is probably better than 0.004%.

4. Results

4.a. $^{40}Ar/^{39}Ar$ dating

The $^{40}Ar/^{39}Ar$ results are given in Table 1 and traditional age spectra are shown in Figure 2. The *c.* 30 fractions of the incremental-heating analyses show only minor variations in apparent age and the two phlogopite separates yield identical 158.5 Ma integrated (total-gas) ages.

Each separate yields a broad age plateau, which is defined as contiguous fractions constituting more than 50% of the total Ar where all fractions overlap with the plateau age within ±2σ. Sample AL/KB21-98 defines a 158.6 ± 0.4 Ma plateau for 89% of the gas, which is from *c.* 7 to 96% cumulative ^{39}Ar released. Sample AL/KB8-98 similarly defines a 158.8 ± 0.4 Ma plateau for 86% of the gas, which is from *c.* 10 to 96% cumulative ^{39}Ar released. The mild discordance among steps is mainly in the small low-temperature fractions (< 750 °C) but also in those of small highest temperature fractions. In addition, all these gas fractions have relatively low K/Ca and K/Cl ratios (see Fig. 2) that indicate impurities associated with the minor age variations in what are otherwise uniform ages from the phlogopite. The 'hump' shape of both spectra is of the type described for talc-bearing

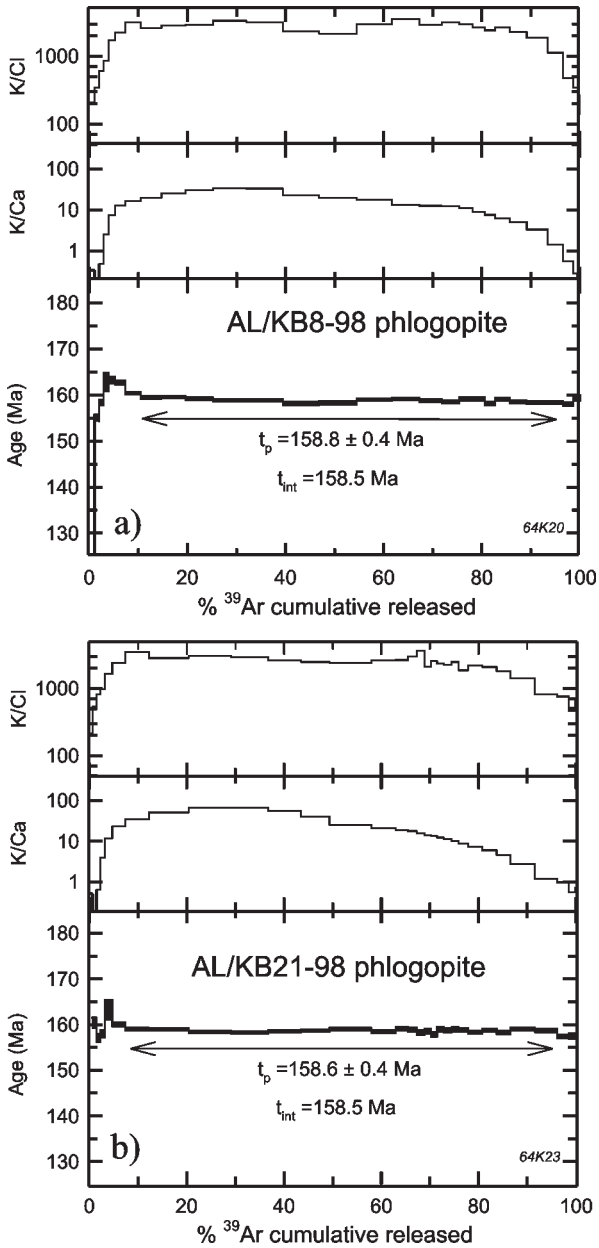

Figure 2. Age spectra for phlogopite from Kjakebeinet lamproite dykes AL/KB8-98 (a) and AL/KB21-98 (b) showing plateaus; t_p is plateau age and t_{int} is the integrated age for the sum of all fractions. The apparent ages are shown with a width corresponding to ± 1σ. See Table 1.

phlogopite by Foland *et al.* (1999) where the internal age variations are due to ^{39}Ar recoil redistribution during irradiation. Since the integrated ages agree with the plateau ages for both samples, the minor discordance in Dronning Maud Land phlogopite could similarly be a recoil artefact arising because of impurities. Whatever the cause, the age spectra yield good plateaus indicating a minimal K/Ar heterogeneity within the phlogopite.

The incremental-heating data were also examined in isotope-correlation analyses with a weighted regression of $^{36}Ar/^{40}Ar$ against $^{39}Ar/^{40}Ar$. For phlogopite

https://doi.org/10.1017/S001675680200674X Published online by Cambridge University Press

Table 2. Geochemical data for Kjakebeinet lamproites and other mafic potassic magmatic rocks

	AL/KB6 –98*	AL/KB8 –98*	AL/KB21 –98*	Leucite Hills †	Priestly Peak ‡	Group II evolved §	Lamproite average **
Major oxides (wt %)							
SiO_2	40.13	40.09	40.18	44.65	50.4	44.87	53.3
TiO_2	4.37	3.98	3.82	2.25	3.52	1.29	3.0
Al_2O_3	8.57	7.88	8.16	8.16	8.95	7.41	9.1
FeO_{tot}	8.75	9.03	10.03	5.74	6.40	7.92	6.3
MnO	0.20	0.20	0.22	0.12	0.10	0.17	0.1
MgO	9.21	12.41	11.49	12.30	8.55	14.89	12.1
CaO	16.24	14.06	12.35	14.06	5.47	10.36	5.8
Na_2O	0.50	0.53	1.32	0.93	0.85	0.83	1.4
K_2O	5.29	5.32	6.16	7.18	8.49	5.52	7.2
P_2O_5	3.81	3.46	3.03	3.04	3.32	0.71	1.3
Sum	97.07	96.96	96.75	98.43	96.05	93.97	99.6
LOI	8.05	7.72	6.71	–	2.62	3.29	5.5
LOI (1200°C) ††	8.40	8.15	7.80	–		–	
Trace elements (ppm)							
Ni	114	269	223	173	300	495	420
Cr	290	373	322	488	362	1239	580
Sc	12	13	16	–	–	11	17
V	200	165	216	–	152	161	123
Ba	4279	3726	4290	5844	10100	2002	5120
Rb	75	105	111	201	284	232	272
Sr	2559	3068	3250	3663	2950	795	1530
Zr	1200	1076	1323	1587	1780	305	922
Y	43	37	37	27	39	11	27
Nb	183	170	166	131	63	54	95
Ga	20	13	15	–	15	–	–
Cu	53	43	52	–	27	25	–
Zn	98	97	115	98	85	60	–
La	263	278	229	347	173	76.0	240
Ce	463	502	408	605	335	149	400
Pr	54.3	59.8	47.1	69.0	–	18.5	–
Nd	208	229	180	258	–	62.2	207
Sm	33.8	36.4	30.0	30.3	–	8.70	24
Eu	9.51	10.0	8.59	6.78	–	2.06	4.8
Gd	22.3	23.0	19.9	16.05	–	6.13	13
Tb	2.83	2.91	2.49	2.00	–	0.59	1.4
Dy	11.1	10.4	9.93	6.48	–	2.27	6.3
Ho	1.71	1.52	1.51	1.15	–	0.36	–
Er	3.42	3.05	3.02	–	–	0.82	–
Tm	0.39	0.34	0.34	–	–	0.11	–
Yb	1.81	1.48	1.64	1.33	–	0.70	1.7
Lu	0.28	0.23	0.24	0.19	–	0.10	0.23
Hf	28.7	26.6	29.2	40.8	–	–	39
Ta	12.4	14.6	11.3	6.52	–	3.95	4.7
Pb	19.1	16.9	19.6	–	28	–	–
Th	21.9	26.1	18.5	37.8	21	8	46
U	3.56	3.32	1.68	8.43	10	1.4	4.9

* Major oxides determined for ignited (1000°C) powders.
† Representative diopside madupitic lamproite from Leucite Hills, Wyoming, USA (sample MAD1; Thompson *et al.* 1984).
‡ Representative lamproite from Priestly Peak, Enderbyland, Antarctica (sample 777283950; Sheraton & England, 1980).
§ Average of three evolved group II kimberlites from Postmasburg (24/PK37), RSA (K. M. Tainton, unpub. Ph.D. thesis, Univ. Cambridge, 1992).
** Average lamproite of Bergman (1987).
†† Loss on ignition at 1200°C; measurements performed at the Geochemical Laboratory, Department of Geology, Univerisity of Helsinki.

AL/KB21-98, the regression of all fractions produces an isotope correlation with a MSWD of 24 giving an age of 158.5 ± 0.5 Ma and a $^{40}Ar/^{36}Ar$ intercept of 298 ± 20. If the discordant 600°C fraction is omitted, the regression (MSWD = 1.5) produces an age of 158.5 ± 0.4 Ma and $^{40}Ar/^{36}Ar$ of 302 ± 5. Regression of all the plateau fractions (MSWD = 0.7) gives an age of 158.6 ± 0.4 Ma and $^{40}Ar/^{36}Ar$ of 303 ± 8. For phlogopite AL/KB8-98, regression of all fractions (MSWD = 151) indicates an age of 158.6 ± 1.0 Ma and $^{40}Ar/^{36}Ar$ of 297 ± 37. Elimination of the small lowest temperature step gives an age of 158.9 ± 0.4 Ma and $^{40}Ar/^{36}Ar$ of 303 ± 9 (MSWD = 7.3), whereas using only the plateau fractions yields an age of 159.3 ± 0.5 Ma and $^{40}Ar/^{36}Ar$ of 254 ± 23 (MSWD = 1.7). The last regression gives an unrealistic $^{40}Ar/^{36}Ar$ intercept, which accounts for the slightly higher and less reliable apparent age from this approach. Otherwise, all the regressions for both samples produce ages that agree with the age spectrum analyses and intercepts

https://doi.org/10.1017/S001675680200674X Published online by Cambridge University Press

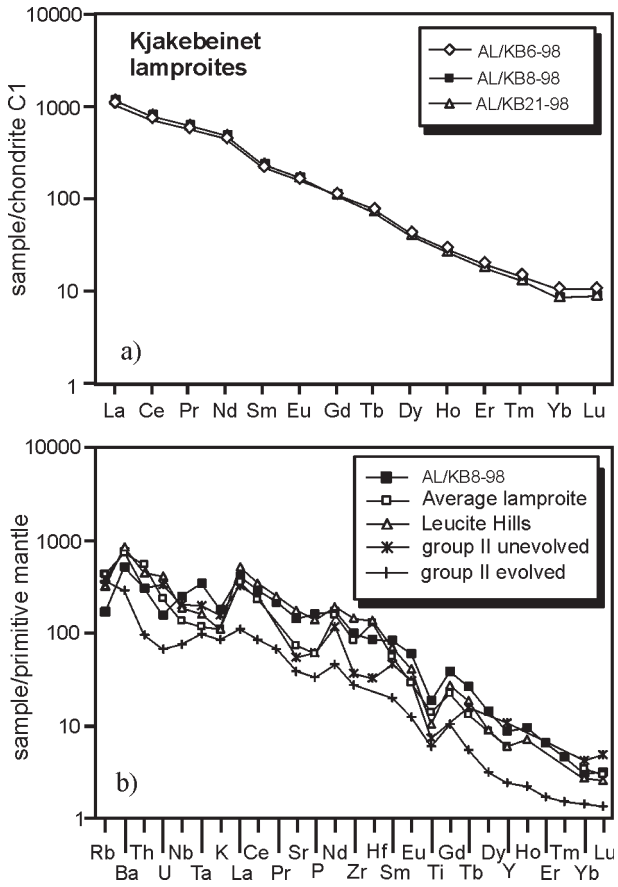

Figure 3. Chondrite-normalized rare earth element diagram (a) and primitive mantle-normalized incompatible element diagram (b) for Kjakebeinet lamproites and selected ultrapotassic rocks. Data sources: Bergman (1987), average lamproite; Thompson *et al*. (1984), Leucite Hills madupitic lamproite; Mitchell (1995*a*), group II (unevolved) kimberlite; K. M. Tainton (unpub. Ph.D thesis, Univ. Cambridge, 1992), evolved group II kimberlite. Normalization values from Sun & McDonough (1989).

indistinguishable from air Ar. The results of the spectrum analysis are adopted because the omitted fractions are those that are anomalous in K/Ca and K/Cl indicating the influence of extraneous phases and because the plateau weights fractions in proportion to the amount of Ar in each.

The plateau ages, 158.6 ± 0.4 Ma and 158.8 ± 0.4 Ma, are not analytically distinct and overlap at the ± 1σ level. The uncertainties on each are appropriate to comparison of these ages, as they include provisions for variations in age among plateau fractions and a relative uncertainty (±0.25%) in determination of the irradiation parameter. Since both phlogopite fractions give indistinguishable dates, the age of the dykes is taken as the average, 158.7 Ma. This age carries a total absolute uncertainty of ± 1.6 Ma when providing for the uncertainty arising from the monitor age.

The 158.7 ± 1.6 Ma phlogopite age is interpreted to represent the cooling of phlogopite below its blocking temperature. Since the dykes would have cooled very rapidly, this age will reflect the time of crystallization. The release spectra and identical ages of the two samples indicate that the phlogopites have not been disturbed by later events or processes.

4.b. Geochemistry

Geochemical data on the Kjakebeinet lamproite dykes are listed in Table 2. The analysed samples are quite similar: they are ultrabasic (SiO_2 40.09–40.18 wt%), ultrapotassic (K_2O 5.29–6.16 wt%, molar K_2O/Na_2O 3.07–6.96), and exhibit low Al_2O_3 relative to total alkalis (molar K_2O/Al_2O_3 0.67–0.82, molar $(K_2O+Na_2O)/Al_2O_3$ 0.76–1.08). Compared to the average lamproite of Bergman (1987), they are notably low in SiO_2 and high in CaO (12.35–16.24 wt%) and P_2O_5 (3.03–3.81 wt%) and, in this respect, are rather similar to diopside madupitic lamproites from Leucite Hills, Wyoming, USA (Table 2). Whereas the latter are clearly lower in TiO_2 than the Kjakebeinet dykes, other lamproites from Antarctica, such as the Priestly Peak lamproites from Enderby Land (Sheraton & England, 1980), have been also noticed for their high TiO_2 and P_2O_5 (Table 2).

The Kjakebeinet lamproite dykes are strongly enriched in incompatible elements with, for example, the ranges of Ba (3726–4290 ppm), Sr (2559–3250 ppm), La (229–278 ppm) and Zr (1076–1323 ppm) being comparable to the average lamproite (Table 2). The dykes have nearly linear chondrite-normalized REE patterns and strong LREE enrichment with La_N values two orders of magnitude higher than those of Lu_N (Fig. 3a). Primitive mantle-normalized incompatible element patterns are grossly linear between Lu and La with the exception of a marked negative Ti anomaly (Fig. 3b). K, Rb and U are strongly, and Th, Nb and Ta moderately to slightly, depleted relative to La and Ba. The overall pattern is atypical of lamproites with respect to higher Sr and P, but it is notably similar to that of some Leucite Hills lamproites.

The sums of oxides for the Kjakebeinet lamproites are low in Table 2. This is in part due to extremely high trace element concentrations (notably Ba, Sr and Zr), which correspond to *c.* 1–1.5 wt% when converted to oxides. The major element analyses were performed using previously ignited (1000 °C) rock powders. Comparison of LOI values measured after ignition at 1000 °C and 1200 °C (Table 2) indicates 0.4–1.1 wt% residual water after ignition at 1000 °C probably due to stability of phlogopite at high temperatures (cf. Hoch, 1999).

4.c. Nd and Sr isotopes

Results of Nd and Sr isotopic analyses are listed in Table 3. Isotopic analyses of the chemically quite similar AL/KB6-98 and AL/KB8-98 dykes yielded notably different compositions. $^{143}Nd/^{144}Nd$ are clearly below bulk earth values with initial ε_{Nd} (159 Ma) values of

https://doi.org/10.1017/S001675680200674X Published online by Cambridge University Press

Table 3. Rb–Sr and Sm–Nd isotopic data for Kjakebeinet lamproites

Sample	Rb*	Sr*	$^{87}Rb/^{86}Sr$ †	$^{87}Sr/^{86}Sr$ ‡	$^{87}Sr/^{86}Sr_T$ §
AL/KB6-98	71.9	2417	0.08572	0.705517±14	0.70532
AL/KB8-98	92.4	2828	0.09416	0.705758±14	0.70555
Sample	Sm*	Nd*	$^{147}Sm/^{144}Nd$ †	$^{143}Nd/^{144}Nd$ ‡	ε_{Nd} (T) §
AL/KB6-98	31.8	222.7	0.08629	0.512219±10	–6.0
AL/KB8-98	33.3	242.1	0.08311	0.512176±11	–6.7

* Concentrations determined by isotope dilution.
† Estimated error for $^{87}Rb/^{86}Sr$ and $^{147}Sm/^{144}Nd$ is less than 0.5%.
‡ $^{143}Nd/^{144}Nd$ normalized to $^{146}Nd/^{144}Nd = 0.7219$, $^{87}Sr/^{86}Sr$ to $^{86}Sr/^{84}Sr = 0.1194$. Within-run error expressed as $2\delta_m$ in the last significant digits.
§ Values reported at 159 Ma. Initial ε_{Nd} calculated using $^{143}Nd/^{144}Nd = 0.51264$ and $^{147}Sm/^{144}Nd = 0.1966$. Maximum error is ±0.3 ε-units.

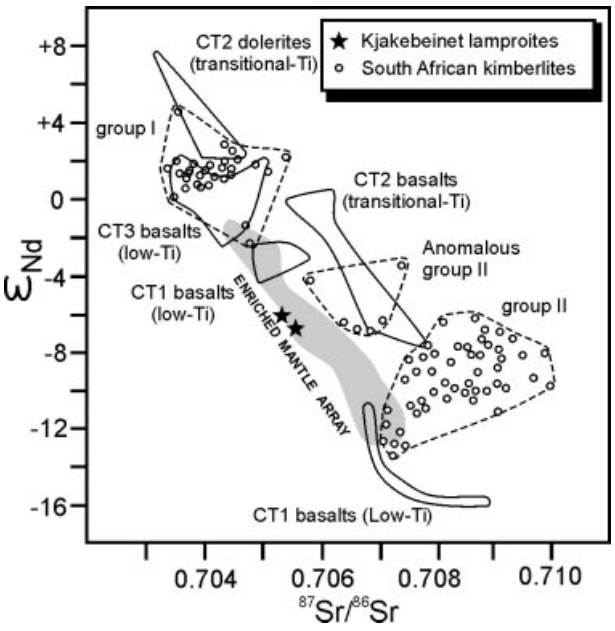

Figure 4. A plot of initial $^{87}Sr/^{86}Sr$ v. ε_{Nd} of Kjakebeinet lamproites. Compositional fields of groups I and II kimberlites, Enriched Mantle Array and Jurassic Vestfjella flood basalts are shown for comparison. CT1, chemical type 1; CT2, chemical type 2; CT3 chemical type 3 (Luttinen & Siivola, 1997). Data sources: Menzies & Murthy (1980), Mitchell (1995*a*), Luttinen, Rämö & Huhma (1998), Luttinen & Furnes (2000).

–6.0 and –6.7. However, the sample with the lower ε_{Nd} value also has slightly lower $^{147}Sm/^{144}Nd$ so that these dykes have similar depleted mantle (T_{DM}) model ages (DePaolo, 1981) of *c.* 1.1 Ga. Low ε_{Nd} are coupled with relatively high initial $^{87}Sr/^{86}Sr$ (0.70532 and 0.70555) so that the samples plot within the Enriched Mantle Array of Menzies & Murthy (1980) and also show affinities to the 20 Ma older low-Ti tholeiites of Vestfjella (Luttinen, Rämö & Huhma, 1998; Luttinen & Furnes, 2000) (Fig. 4).

5. Discussion

5.a. Relationship to group II kimberlites of southern Africa

Previously, lamproites have been reported at only three localities in Antarctica (Mitchell & Bergman, 1991). All of these localities are situated far from western Dronning Maud Land. Prior to the Jurassic breakup of Gondwana, western Dronning Maud Land was juxtaposed to southeastern Africa, where mica-rich group II kimberlites (orangeites: Mitchell, 1995*a*) record Mesozoic potassic–ultrapotassic magmatism. Group II kimberlites are, in many respects, different from archetypal group I kimberlites, but quite similar to lamproites (Mitchell, 1995*a*). The group II kimberlite fields that were generated during a considerable period of time between 200 and 110 Ma (Skinner, 1989) comprise a scattered, broadly NE-trending belt, which extends across the Kaapvaal Craton towards western Dronning Maud Land in Gondwana reconstruction at 180 Ma (Fig. 5).

Mineralogical, geochemical and isotopic comparison suggests that the Kjakebeinet lamproites have some transitional features between lamproites and group II kimberlites. Assemblages of olivine, diopside, phlogopite and sanidine are common in both rock types (Mitchell, 1997). However, Ti-rich phlogopite–tetraferriphlogopite, such as in the Kjakebeinet lamproites, is only typical of lamproites, whereas monazite and abundant carbonate are more typical of group II kimberlites (Mitchell & Bergman, 1991; Mitchell, 1995*a*). Geochemically, the Kjakebeinet lamproites differ clearly from most group II kimberlites based on notably higher MgO and lower K_2O in the latter (cf. Mitchell, 1995*a*). Such MgO-rich group II kimberlites have similar REE, but lower Ti, P, Zr and Hf contents than the Kjakebeinet lamproites (Fig. 3b; Mitchell, 1995*a*). Evolved group II kimberlites include rocks with broadly similar major element compositions to those of the Kjakebeinet lamproites (Table 2). Although the concentrations of TiO_2 and P_2O_5 and incompatible trace elements are clearly lower in these kimberlites, the overall resemblance of the mantle-normalized incompatible element patterns indicate quite similar incompatible element ratios (Fig. 3b). The initial ε_{Nd} values of the Kjakebeinet lamproites overlap with those of some group II kimberlites, whereas the initial Sr isotopic ratios are somewhat lower (Fig. 4).

The origin of lamproites, group II kimberlites and other mafic potassic rock types has been widely ascribed to melting of phlogopite-bearing metasome

https://doi.org/10.1017/S001675680200674X Published online by Cambridge University Press

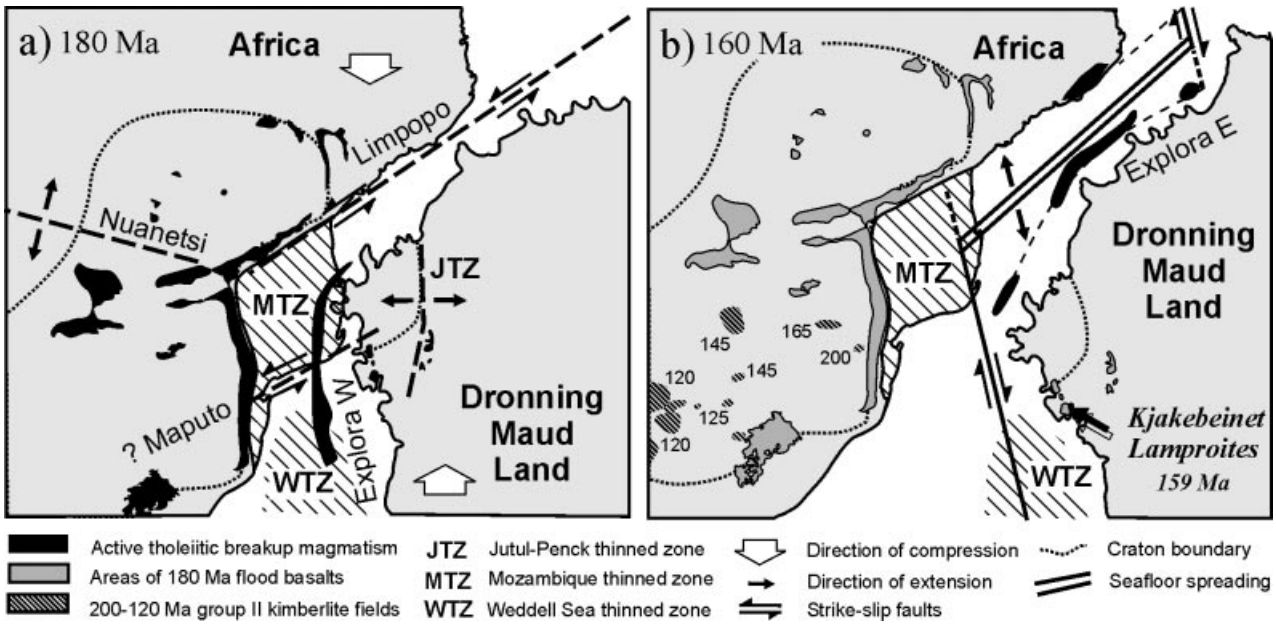

Figure 5. Schematic presentation of Gondwana breakup (modified after Cox, 1992). (a) Stage 1 at 180 Ma: Emplacement of continental flood basalts and western Explora (black) in association with lithospheric extension in western Dronning Maud Land and development of Mozambique thinned zone (MTZ), Weddell Sea thinned zone (WTZ), and Jutul-Penck thinned zone (JTZ). (b) Stage 2 at 160 Ma: Emplacement of eastern Explora and Kjakebeinet lamproites in association with early seafloor spreading between Africa and Antarctica and transform faulting within the Mozambique–Weddell Sea thinned zone. Distribution of group II kimberlite fields in Africa (ages indicated) is shown in (b). Reconstruction at 160 Ma is after Lavwer, Gahagan & Coffin (1992).

veins in the lithospheric mantle (e.g. Bergman, 1987; Foley *et al.* 1987; McKenzie, 1989; Rock, 1991; Mitchell, 1995*b*; Leat *et al.* 1999). Group II kimberlites have been considered to represent a distinct magma type that is unique to southern Africa. Their genesis has been related to the long-term evolution of the lithospheric mantle beneath the Kaapvaal Craton (Tainton & McKenzie, 1994; Mitchell, 1995*a*), which has involved infiltration of highly LREE-enriched fluids and/or melts from asthenosphere during the Proterozoic time, possibly at approximately 1.2 Ga during the Namaqua orogeny (Richardson *et al.* 1984; Walker *et al.* 1989; K. M. Tainton, unpub. Ph.D. thesis, Univ. Cambridge, 1992).

The pre-breakup proximity of southeastern Africa and western Dronning Maud Land, coupled with isotopical, chemical and mineralogical affinities between the Kjakebeinet lamproites and group II kimberlites, suggest that these rocks could have been derived from broadly similar lithospheric mantle sources. Moreover, *c.* 114 Ma old alkaline rocks in the Damodar Valley, eastern India, also exhibit affinities to group II kimberlites (Kent, Kelley & Pringle, 1998). The data from Dronning Maud Land and the Damodar Valley thus imply that a compositionally distinctive Gondwanan lithospheric mantle domain may have extended from southern Africa across Dronning Maud Land to India. On the other hand, a recent report of Proterozoic group II kimberlite equivalents from Finland shows that suitable conditions for generation of group II kimberlite-like rocks have also developed within other cratons at different times (O'Brien & Tyni, 1999).

5.b. Implications for mantle source regions

It is probable that many, if not most, mafic potassic rocks represent hybrids of lithospheric vein-derived melts and xenocrystic wall-rock mantle material (Mitchell & Bergman, 1991) or basaltic magma from asthenosphere (O'Brien, Irving & McCallum, 1991). The Kjakebeinet lamproites are among the most incompatible element-enriched rocks worldwide. Because of their extremely high Nd and Sr concentrations (> 200 ppm and > 2000 ppm, respectively), the isotopic ratios of the Kjakebeinet lamproites have been effectively buffered against crustal contamination or possible mixing with asthenosphere-derived basaltic magmas. Assuming that the Kjakebeinet lamproite dykes represent partial melts of lithospheric metasome veins and that their Nd isotopic compositions and Sm/Nd are unaffected by contamination and subsolidus alteration, their T_{DM} Nd model ages point to mantle enrichment in western Dronning Maud Land having occurred at or prior to *c.* 1.1 Ga. This age corresponds to the main orogenic period along the Maud Belt (Arndt *et al.* 1991; Fig. 1b) and adds to geological links between western Dronning Maud Land and southeastern Africa.

Overall, the isotopic data on mantle xenoliths, kimberlites and the Kjakebeinet lamproites define a broad

https://doi.org/10.1017/S001675680200674X Published online by Cambridge University Press

array that provides the best available estimate of the composition of upper mantle beneath the Karoo large igneous province in Jurassic time. This 'mantle array' extends from asthenospheric (group I kimberlites) to lithospheric compositions and coincides with the fields of different flood basalt types of Vestfjella (Fig. 4), which lends support to the view that the latter record mixing of asthenospheric and lithospheric mantle material (Luttinen & Furnes, 2000).

5.c. Implications for early breakup

Generation of mafic potassic melts is a likely consequence of extension and/or heating of the lithosphere during the initial stage of continental breakup (e.g. McKenzie, 1989; Thompson *et al.* 1989). Many petrogenetic models of flood basalts assume that production of potassic magma continues during the peak of tholeiitic magmatism and leads to mixing between lithospheric and asthenospheric melts. Leat *et al.* (1999) have reported a possible example of coeval potassic and tholeiitic magmatism in the case of the Ferrar large igneous province.

Various case studies indicate that continental flood basalts may contain from a few to up to 50 percent of a potassic component (Ellam & Cox, 1991; Ellam, Carlson & Shirley, 1992; Cadman, Tarney & Baragar, 1995; Gibson *et al.* 1996; Luttinen & Furnes, 2000), although the highest values seem unrealistic considering the small proportion of metasome vein material in the lithosphere and the huge volumes of presumably lithosphere-contaminated basalts. Wholesale melting of metasomatized lithospheric mantle is also a widely supported petrogenetic model for the voluminous low-Ti tholeiites (Hawkesworth *et al.* 1984; Hergt, Peate & Hawkesworth, 1991; Gallagher & Hawkesworth, 1992; Sweeney, Duncan & Erlank, 1994). It seems inevitable that voluminous flood basalt magmatism effectively depletes metasomatized peridotite of fusible material. The discovery of post-flood basalt lamproites in Vestfjella raises the question of how apparently old, easily fusible material could have survived in a region that was previously underlain by a large and hot mantle plume head and where great volumes of basalt magmas have passed through and possibly were even generated within the lithosphere (cf. Gibson *et al.* 1999).

Several studies have proposed that the production and emplacement of flood basalt magmas are not evenly distributed over a large plume head. These processes may be controlled by the topography of the base of the lithosphere and development of active zones of lithospheric thinning (e.g. White & McKenzie, 1989; Ebinger & Sleep 1998; Thompson & Gibson, 1991). Zones of relatively thin lithosphere may help to channel the thermal anomaly and facilitate high melt production in upwelling mantle and also favour emplacement of generated magmas through deep-seated fault systems. During the early stages of rift initiation, these lithospheric rupture zones may have been steep and narrow (Nicholas, Achauer & Daignieres, 1994). Thus, if narrow zones of previously thinned or actively thinning lithosphere had a controlling influence on the generation and emplacement of flood basalts in Dronning Maud Land at *c.* 180 Ma, as suggested by Luttinen & Furnes (2000), a metasomatized source for Kjakebeinet lamproite dykes could have survived directly beneath Vestfjella, between the Weddell Sea and Jutul-Penck zones of thinning (Fig. 5a).

5.d. Implications for late breakup events

As in Dronning Maud Land, mafic potassic magmatism in the Paraná province significantly post-dates eruption of flood basalts. Gibson *et al.* (1999) viewed this as evidence against wholesale melting of lithospheric mantle during flood basalt magmatism, and ascribed post-flood basalt potassic magmatism to melting of metasomatically enriched mantle lithosphere as a consequence of the impact of a second mantle plume beneath South America. Similarly, le Roex (1986) and Skinner (1989) have suggested that the array of group II kimberlite fields (Fig. 5b) records a hot spot trail across southern Africa. Bailey (1993) and Mitchell (1995*a*) have opposed this idea and the latter has considered that these fields were generated during two separate events at 125–110 Ma (the main cluster near the southwestern part of the craton) and 165–145 Ma (in the central part of the craton). According to Mitchell (1995*a*), the 200 Ma age for the intrusion adjacent to Lebombo monocline requires reinvestigation. In tight Gondwana reconstructions (Fig. 1a), Vestfjella is located quite near to the 165 Ma cluster of group II kimberlites. However, Antarctica had started to rift apart from Africa at 160 Ma (Lawver, Gahagan & Coffin, 1992) and, although the plate movements during 180–160 Ma are imprecisely known, there may have been a distance of over 1000 km between the two continents (Fig. 5b). Coeval ultrapotassic intrusions in southeastern Africa and Dronning Maud Land thus probably relate to different tectonomagmatic systems.

According to the model presented by Cox (1992), the breakup between Africa and Antarctica involved two separate stages. After the short period of flood basalt magmatism at *c.* 180 Ma (Stage 1), Vestfjella was located adjacent to a region of strongly extended lithosphere (Weddell Sea–Mozambique thinned zone, Fig. 5a). The next major event in this region was probably associated with the final breakup between Africa and Antarctica (Stage 2) that, on the basis of the oldest discovered sea floor, may have started at *c.* 160 Ma. In western Dronning Maud Land, the period has been associated with a change from E–W stretching to coast-parallel strike-slip faulting (Fig. 5b), but the transition has been geologically undocumented.

https://doi.org/10.1017/S001675680200674X Published online by Cambridge University Press

The 159 Ma Kjakebeinet lamproite dykes can be temporally and spatially associated with the Stage 2 of the Cox (1992) breakup model. Field observations demonstrate abundant normal faulting in Vestfjella, but do not indicate significant lateral displacements that should characterize Stage 2 of breakup in this region. However, it is difficult to recognize small-scale lateral displacements in the small rock outcrops of Vestfjella due to intensive normal faulting and abundant loose cover. Moreover, major shear zones are likely to be topographic depressions presently buried under the East Antarctic ice sheet.

Recent dating by Ar–Ar and U–Pb methods supports rapid emplacement of flood basalts in the Karoo and Ferrar provinces at *c.* 180 ± 3 Ma (Heimann *et al.* 1994; Encarnación *et al.* 1996; Fleming *et al.* 1997; Duncan *et al.* 1997; X. Zhang, pers. comm., 2002). There is no evidence of basaltic magmatism associated with the 165–110 Ma ultrapotassic magmatism. It is therefore unlikely that the Kjakebeinet lamproites record mobilization of old lithospheric material due to intrusion of asthenosphere-derived basalt magma through the lithospheric mantle. However, potassic magmatism has been associated with oceanic and continental shear zones (Weijermars, 1987; McNeil & Kerrich, 1986; McHone, Ross & Greenough, 1987; da Silva Filho, Thompson & Leat, 1987; Jones *et al.* 1991). More specifically, transtension generated in a strike-slip fault may be sufficient to trigger incipient melting of metasomatized mantle (Vaughan, 1996). The major fault zone during Stage 2 was within the previously thinned lithospheric zone to the west of Dronning Maud Land that subsequently subsided below sea-level. It seems possible that adjacent to the major shear zone, the lithospheric mantle beneath Vestjella could have been involved in strike-slip faulting related to initial seafloor spreading. We envisage that, adapting from the model of Vaughan (1996), deep and steep transform faults, associated with the late breakup of Gondwana, first triggered production of lamproite magmas and then provided conduits into which these magmas were emplaced.

6. Conclusions

(1) The mica-rich mafic dykes from Kjakebeinet can be classified as lamproites.

(2) Based on $^{40}Ar/^{39}Ar$ dating of phlogopite, the Kjakebeinet lamproites were emplaced at 158.7 ± 1.6 Ma and thus post-date the associated flood basalts by *c.* 20 Ma.

(3) The ultrapotassic compositions, low initial ε_{Nd} values of –6.0 and –6.7, and Nd T_{DM} model ages of 1.1 Ga suggest an old metasomatized lithospheric mantle source for the lamproite magmas. Compositional similarities indicate that the source was broadly similar to that of group II kimberlites of southern Africa.

(4) Dyke emplacement was contemporaneous with the late-stage breakup between East and West Gondwana and, following the two-stage breakup model of Cox (1992), can be linked to strike-slip faulting near the continental margin of western Dronning Maud Land. Deep strike-slip faulting may have facilitated lamproite magma formation and emplacement.

(5) Emplacement of lamproites *c.* 20 Ma after flood basalt eruptions indicates that parts of the metasomatized lithospheric mantle have remained intact during flood basalt magmatism. This lends support to a controlling influence for lithospheric rifting zones on continental flood basalt generation and emplacement.

Acknowledgements. We wish to thank Mika Räisänen for assistance in the fieldwork, Hannu Huhma and Arto Pulkkinen for their help in the radiogenic isotope analyses, Lassi Pakkanen for microprobe analyses, Fritz Hubacher for laboratory support with the argon analyses, Jeff Linder and Frank Huffman for help with construction and maintenance of the argon mass analysis facilities, and staff of the Ford Reactor at the University of Michigan for sample irradiations. Comments by David Elliot, Hugh O'Brien, Philip Leat, Alan Vaughan and the journal referees Andy Saunders and Brian Storey significantly improved the manuscript. AVL has been funded by Academy of Finland (Grant 43922). XZ and KAF acknowledge support from National Science Foundation grant OPP-9527816 and National Science Foundation equipment grant EAR-9220344.

References

Arndt, N. T., Todt, W., Chauvel, M., Tapfer, M. & Weber, K. 1991. U–Pb zircon age and Nd isotopic composition of granitoids, charnockites and supracrustal rocks from Heimefrontfjella, Antarctica. *Geologische Rundschau* **80**, 759–77.

Bailey, D. K. 1993. Petrogenetic implications of the timing of alkaline, carbonatite and kimberlite igneous activity in Africa. *South African Journal of Geology* **96**, 67–74.

Bergman, S. C. 1987. Lamproites and other potassium-rich igneous rocks: a review of their occurrence, mineralogy and geochemistry. In *Alkaline Igneous Rocks* (eds J. G. Fitton and B. G. J. Upton), pp. 103–90. Geological Society of London, Special Publication no. 30.

Cadman, A. C., Tarney, J. & Baragar, W. R. A. 1995. Nature of mantle source contributions and the role of contamination and in situ crystallization in the petrogenesis of Proterozoic mafic dykes and flood basalts in Labrador. *Contributions to Mineralogy and Petrology* **122**, 213–29.

Cox, K. G. 1992. Karoo igneous activity, and the early stages of the break-up of Gondwanaland. In *Magmatism and the Causes of Continental Break-up* (eds B. C. Storey, T. Alabaster and R. J. Pankhurst), pp. 137–48. Geological Society of London, Special Publication no. 68.

da Silva Filho, A. F., Thompson, R. N. & Leat, P. T. 1987. Petrology of Terra Nova pluton, Brazil, and associated ultrapotassic dykes. *Revista Brasileira de Geociências* **17**, 481–7.

DePaolo, D. J. 1981. Neodymium isotopes in the Colorado Front range and crust–mantle evolution in the Proterozoic. *Nature* **291**, 193–6.

Duncan, R. A., Hooper, P. R., Rehacek, J., Marsh, J. S. &

Duncan, A. R. 1997. The timing and duration of the Karoo igneous event, southern Gondwana. *Journal of Geophysical Research* **102**, 18127–38.

Ebinger, C. J. & Sleep, N. H. 1998. Cenozoic magmatism throughout east Africa resulting from impact of a single plume. *Nature* **395**, 788–91.

Ellam, R. M., Carlson, R. W. & Shirley, S. B. 1992. Evidence from Re–Os isotopes for plume-lithosphere mixing in Karoo flood basalt genesis. *Nature* **359**, 718–21.

Ellam, R. M. & Cox, K. G. 1991. An interpretation of Karoo picrite basalts in terms of interaction between asthenospheric magmas and the mantle lithosphere. *Earth and Planetary Science Letters* **105**, 330–42.

Encarnación, J., Fleming, T. H., Elliot, D. H. & Eales, H. V. 1996. Synchronous emplacement of Ferrar and Karoo dolerites and the early breakup of Gondwana. *Geology* **24**, 535–8.

Fleming, T. H., Heimann, A., Foland, K. A. & Elliot, D. H. 1997. $^{40}Ar/^{39}Ar$ geochronology of Ferrar Dolerite sills from the Transantarctic Mountains, Antarctica: implications for the age and origin of the Ferrar magmatic province. *Geological Society of America Bulletin* **109**, 533–46.

Foland, K.A., Fleming, T. H., Heimann, A. & Elliot, D. H. 1993. Potassium–argon dating of fine-grained basalts with massive Ar loss: Application of $^{40}Ar/^{39}Ar$ technique to plagioclase and glass from Kirkpatrick Basalt, Antarctica. *Chemical Geology* **107**, 173–90.

Foland, K. A., Zhang, X., Hubacher, F. & Dahl, P. S. 1999. Recoil-induced $^{40}Ar/^{39}Ar$ age discordance in phlogopite. *Abstracts with Programs, Geological Society of America* **31**(7), A345.

Foley, S. F., Venturelli, G., Green, D. H. & Toscani, L. 1987. The ultrapotassic rocks: characteristics, classification, and constraints for petrogenetic models. *Earth Science Reviews* **24**, 81–134.

Gallagher, K. & Hawkesworth, C. J. 1992. Dehydration melting and the generation of continental flood basalts. *Nature* **358**, 57–9.

Gibson, S. A., Thompson, R. N., Dickin, A. P. & Leonardos, O. H. 1996. High-Ti and low-Ti mafic potassic magmas: key to plume–lithosphere interactions and flood basalt genesis. *Earth and Planetary Science Letters* **141**, 325–41.

Gibson, S. A., Thompson R. N., Leonardos, O. H., Dickin, A. P. & Mitchell, J. G. 1999. The limited extent of plume-lithosphere interactions during continental flood-basalt genesis: geochemical evidence from Cretaceous magmatism in southern Brazil. *Contributions to Mineralogy and Petrology* **137**, 147–69.

Gradstein, F. M., Agterberg, F. P., Ogg, J. G., Hardenbol, J., van Veen, P., Thierry, J. & Huang, Z. 1995. A Triassic, Jurassic and Cretaceous time scale. In *Geochronology, Time Scales, and Global Stratigraphic Correlation* (eds W. A. Bergren, D. V. Kent, M-P. Aubry and J. Hardenbol), pp. 95–126. Society of Economic Paleontologists and Mineralogists, Special Publication no. 54.

Grantham, G. H. 1996. Aspects of Jurassic magmatism and faulting in western Dronning Maud Land, Antarctica: implications for Gondwana break-up. In *Weddell Sea Tectonics and Gondwana Break-up* (eds B. C. Storey, E. C. King and R. A. Livermore), pp. 63–73. Geological Society of London, Special Publication no. 108.

Grind, K. H., Luttinen, A. V. & Siivola, J. U. 1991. A geological overview of the Vestfjella mountains in western Dronning Maud Land, Antarctica. *Antarctic Reports of Finland* **1**, 11–15.

Groenewald, P. M., Moyes, A. B., Grantham, G. H. & Krynauw, J. R. 1995. East Antarctic crustal evolution: geological constraints and modelling in western Dronning Maud Land. *Precambrian Research* **75**, 231–50.

Harris, C. & Grantham, G. H. 1993. Geology and petrogenesis of the Straumsvola nepheline syenite complex, Dronning Maud Land, Antarctica. *Geological Magazine* **130**, 513–32.

Harris, C., Marsh, J. S., Duncan, A. R. & Erlank, A. J. 1990. The petrogenesis of the Kirwan Basalts of Dronning Maud Land, Antarctica. *Journal of Petrology* **31**, 341–69.

Harris, C., Watters, B. R. & Groenewald, P. B. 1991. Geochemistry of the Mesozoic regional basic dykes of western Dronning Maud Land, Antarctica. *Contributions to Mineralogy and Petrology* **107**, 100–11.

Hawkesworth, C. J., Marsh, J. S., Duncan, A. R., Erlank, A. J. & Norry, M. J. 1984. The role of continental lithosphere in the generation of the Karoo volcanic rocks: evidence from combined Nd- and Sr-isotpe studies. In *Petrogenesis of the volcanic rocks of the Karoo Province* (ed. A. J. Erlank), pp. 341–54. Geological Society of South Africa, Special Publication no. 13.

Heimann, A., Fleming, T. H., Elliot, D. H. & Foland, K. A. 1994. A short interval of Jurassic continental flood basalt volcanism in Antarctica as demonstrated by $^{40}Ar/^{39}Ar$ geochronology. *Earth and Planetary Science Letters* **121**, 19–41.

Hergt, J. M., Peate, D. W. & Hawkesworth, C. J. 1991. The petrogenesis of Mesozoic Gondwana low-Ti flood basalts. *Earth and Planetary Science Letters* **105**, 134–48.

Hoch, M. 1999. Geochemistry and petrology of ultramafic lamprophyres from Schirmacher Oasis, East Antarctica. *Mineralogy and Petrology* **65**, 51–67.

Jacobs, J., Thomas, R. J. & Weber, K. 1993. Accretion and indentation tectonics at the southern edge of the Kaapvaal craton during Kibaran (Grenville) orogeny. *Geology* **21**, 203–6.

Johnson, D. M., Hooper, P. R. & Conrey, R. M. 1999. XRF analysis of rocks and minerals for major and trace elements on a single low dilution Li-tetraborate fused bead. *Advances in X-ray Analysis* **41**, 843–67.

Jones, E. J. W., Goddard, D. A., Mitchell, J. G. & Banner, F. T. 1991. Lamprophyric volcanism of Cenozoic age on the Sierra Leone Rise: implications for regional tectonics and the stratigraphic time scale. *Marine Geology* **99**, 19–28.

Juckes, L. M. 1972. The geology of northeastern Heimefrontfjella, Dronning Maud Land. *British Antarctic Survey Scientific Reports* **65**, 44 pp.

Kent, R. W., Kelley, S. P. & Pringle, M. S. 1998. Mineralogy and $^{40}Ar/^{39}Ar$ geochronology of orangeites (Group II kimberlites) from the Damodar Valley, eastern India. *Mineralogical Magazine* **62**, 313–23.

Knaack, C., Cornelius, S. & Hooper, P. 1994. *Trace element analyses of rocks and minerals by ICP-MS.* Department of Geology, Washington State University.

Lawver, L. A., Gahagan, L. M. & Coffin, M. F. 1992. The development of paleoseaways around Antarctica. In

https://doi.org/10.1017/S001675680200674X Published online by Cambridge University Press

The Antarctic paleoenvironment, a perspective on global change (eds J. P. Kennett and D. A. Warnke), pp. 7–30. Antarctic Research Series no. 56.

LE ROEX, A. P. 1986. Geochemical correlations between southern African kimberlites and south Atlantic hot spots. *Nature* **324**, 243–5.

LEAT, P. T., RILEY, T. R., STOREY, B. C., KELLEY, S. P. & MILLAR, I. L. 1999. Middle Jurassic ultramafic lamprophyre dyke within the Ferrar magmatic province, Pensacola Mountains, Antarctica. *Mineralogical Magazine* **64**, 95–111.

LIVERMORE, R. A. & HUNTER, R. J. 1996. Mesozoic seafloor spreading in the southern Weddell Sea. In *Weddell Sea Tectonics and Gondwana Break-up* (eds B. C. Storey, E. C. King and R. A. Livermore), pp. 227–41. Geological Society of London, Special Publication no. 108.

LUTTINEN, A. V. & FURNES, H. 2000. Flood basalts of Vestfjella: Jurassic magmatism across an Archaean–Proterozoic lithospheric boundary in Dronning Maud Land, Antarctica. *Journal of Petrology* **41**, 1271–1305.

LUTTINEN, A.V., RÄMÖ, O. T. & HUHMA, H. 1998. Nd and Sr isotopic and trace element composition of a Mesozoic CFB suite from Dronning Maud Land, Antarctica: Implications for lithosphere and asthenosphere contributions to Karoo magmatism. *Geochimica et Cosmochimica Acta* **62**, 2701–14.

LUTTINEN, A. V. & SIIVOLA, J. U. 1997. Geochemical characteristics of Mesozoic lavas and dikes from Vestfjella, Dronning Maud Land: recognition of three distinct chemical types. In *The Antarctic Region: Geological Evolution and Processes* (ed. C. A. Ricci), pp. 495–503. Terra Antarctica Publications.

MCKENZIE, D. 1989. Some remarks on the movement of small melt fractions in the mantle. *Earth and Planetary Science Letters* **95**, 53–72.

MCHONE, J. G., ROSS, M. E. & GREENOUGH, J. D. 1987. Mesozoic dyke swarms of eastern North America. In *Mafic Dyke Swarms* (eds H. C. Halls and W. F. Fahrig), pp. 279–88. Geological Association of Canada, Special Paper no. 34.

MCNEIL, A. M. & KERRICH, R. 1986. Archaean lamprophyre dykes and gold mineralization, Matheson, Ontario: the conjunction of REE-enriched mafic magmas, deep crustal structures and Au concentration. *Canadian Journal of Earth Science* **23**, 324–43.

MENZIES, M. A. & MURTHY, V. M. 1980. Enriched mantle: Nd and Sr isotopes in diopsides from kimberlite nodules. *Nature* **283**, 634–6.

MITCHELL, R. H. 1995*a*. *Kimberlites, Orangeites, and Related Rocks*. New York: Plenum Press, 410 pp.

MITCHELL, R. H., 1995*b*. Melting experiments on a sanidine phlogopite lamproite at 4–7 Gpa and their bearing on the sources of lamproitic magmas. *Journal of Petrology* **36**, 1455–74.

MITCHELL, R. H. 1997. *Kimberlites, Orangeites, Lamproites, Melilites, and Minettes: A Petrographical Atlas*, 1st ed. Thunder Bay: Almaz Press Inc., 242 pp.

MITCHELL, R. H. & BERGMAN, S. C. 1991. *Petrology of Lamproites*. New York: Plenum Press, 447 pp.

NICOLAS, A., ACHAUER, U. & DAIGNIERES, M. 1994. Rift initiation by lithospheric rupture. *Earth and Planetary Science Letters* **123**, 281–98.

O'BRIEN, H. E. & TYNI, M. 1999. Mineralogy and geochemistry of kimberlites and related rocks from Finland. In *Proceedings of the 7th International Kimberlite Conference, Vol 2: L–Z* (eds J. J. Gurney, J. L. Gurney, M. D. Pascoe and S. H. Richardson), pp. 625–36. Cape Town: Red Roof Design.

O'BRIEN, H. E., IRVING, A. J. & MCCALLUM, I. S. 1991. Eocene potassic magmatism in the Highwood Mountains, Montana: petrology, geochemistry and tectonic implications. *Journal of Geophysical Research* **96**, 13237–60.

PETERS, M., 1989. *Die Vulkanite im westlichen und mittleren Neuschwabenland, Vestfjella und Ahlmannryggen, Antarktika.* Berichte zur Polarforschung, Alfred Wegener-Institut für Polar- und Maareforschung, Bremerhaven, 186 pp.

RABINOWITZ, P. D., COFFIN, M. R. & FALVEY, D. 1983. The Separation of Madagascar and Africa. *Science* **220**, 67–9.

RICHARD, P., SHIMIZU, N. & ALLÈGRE, C. J. 1976. $^{143}Nd/^{144}Nd$, a natural tracer: An application to oceanic basalts. *Earth and Planetary Science Letters* **31**, 269–78.

RICHARDSON, S. H., GURNEY, J. J., ERLANK, A. J. & HARRIS, J. W. 1984. Origin of diamonds in old enriched mantle. *Nature* **310**, 198–202.

ROCK, N. M. S. 1991. *Lamprophyres*. Glasgow: Blackie and Son Ltd, 285 pp.

ROESER, H. A., FRITSCH, J. & HINZ, K. 1996. The development of the crust off Dronning Maud Land, East Antarctica. In *Weddell Sea Tectonics and Gondwana Break-up* (eds B. C. Storey, E. C. King and R. A. Livermore), pp. 243–264. Geological Society of London, Special Publication no. 108.

SHERATON, J. W. & ENGLAND, R. N. 1980. Highly potassic mafic dykes from Antarctica. *Journal of the Geological Society of Australia* **27**, 129–35.

SKINNER, E. M. 1989. Contrasting group I and group II kimberlite petrology: towards a genetic model for kimberlites. In *Proceedings of the Fourth International Kimberlite Conference. Kimberlites and Related Rocks. Vol. 1. Their Composition, Occurrence, Origin and Emplacement* (eds J. Ross, A. L. Jaques, J. Ferguson, D. H. Green, S. Y. O'Reilly, R. V. Danchin and A. J. A. Janse), pp. 528–44. Geological Society of Australia, Special Publication no. 14.

SPAETH, G. & SCHÜLL, P. 1987. A survey of Mesozoic dolerite dikes from western Neuschwabenland, Antarctica, and their geotectonic significance. *Polarforschung* **57**, 93–113.

SUN, S. S. & MCDONOUGH, W. F. 1989. Chemical and isotopic systematics of oceanic basalts: implications for mantle composition and processes. In *Magmatism in Ocean Basins* (eds A. D. Saunders and M. J. Norry), pp. 313–45. Geological Society of London, Special Publication no. 42.

SWEENEY, R. J., DUNCAN, A. R. & ERLANK, A. J. 1994. Geochemistry and petrogenesis of Central Lebombo basalts of the Karoo Igneous Province. *Journal of Petrology* **35**, 95–125.

TAINTON, K. M. & MCKENZIE, D. 1994. The generation of kimberlites, lamproites, and their source rocks. *Journal of Petrology* **35**, 787–817.

THOMPSON, R. N. & GIBSON, S. A. 1991. Subcontinental mantle plumes, hotspots and pre-existing thinspots. *Journal of the Geological Society, London* **148**, 973–7.

THOMPSON, R. N., LEAT, P. T., DICKIN, A. P., MORRISON, M. A., HENDRY, G. L. & GIBSON, S. A. 1989. Strongly potassic mafic magmas from lithospheric mantle sources during continental extension and heating: evidence from Miocene minettes of northwest Colorado, U.S.A. *Earth and Planetary Science Letters* **98**, 139–53.

THOMPSON, R. N., MORRISON, M. A., HENDRY, G. L. & PARRY, S. J. 1984. An assessment of the relative roles of crust and mantle in magma genesis: an elemental approach. *Philosophical Transactions, Royal Society of London* **A 310**, 549–90.

VAUGHAN, A. P. M. 1996. A tectonomagmatic model for the genesis and emplacement of Caledonian calc-alkaline lamprophyres. *Journal of the Geological Society, London* **153**, 613–23.

WALKER, R. J., CARLSON, R. W., SHIRLEY, S. B. & BOYD, F. R. 1989. Osmium, strontium, neodymium, and lead isotope systematics of southern African peridotite xenoliths: implications for the chemical evolution of subcontinental mantle. *Geochimica et Cosmochimica Acta* **53**, 1583–95.

WEIJERMARS, R. 1987. The Palomares brittle-ductile shear zone of southern Spain. *Journal of Structural Geology* **9**, 139–57.

WHITE, R. S. & MCKENZIE, D. 1989. Magmatism at rift zones: The generation of volcanic continental margins and flood basalts. *Journal of Geophysical Research* **94**, 7685–7729.

WOLMARANS, L. G. & KENT, L. E. 1982. Geological investigations in western Dronning Maud Land, Antarctica – a synthesis. *South African Journal of Antarctic Research*, Supplement 2, 93 pp.

WOOLLEY, A. R., BERGMAN, S. C., EDGAR, A. D., LEBAS, M. J., MITCHELL, R. H., ROCK, N. M. S. & SCOTT SMITH, B. H. 1996. Classification of lamprophyres, lamproites, kimberlites, and the kalsilitic, melilitic, and leucitic rocks. *The Canadian Mineralogist* **34**, 175–86.

https://doi.org/10.1017/S001675680200674X Published online by Cambridge University Press